



Cyclophosphamide treatment modifies the thermal stability of profilin bound monomeric and leiomodins2 bound filamentous actin

Dávid Szatmári¹ · Beáta Bugyi¹ · Réka Pintér¹ · Dénes Lőrinczy¹

Received: 4 June 2022 / Accepted: 23 September 2022 / Published online: 5 December 2022
© The Author(s) 2022

Abstract

The monomeric (G-actin) and polymer (F-actin) forms of actin play important role in muscle development and contraction, cellular motility, division, and transport processes. Leiomodins 1–3 (Lmod1–3) are crucial for the development of muscle sarcomeres. Unlike tropomodulins that localize only at the pointed ends, the striated muscle specific Lmod2 shows diffuse distribution along the entire length of the thin filaments. The G-actin-binding profilin (Pro) facilitates the nucleotide exchange on monomeric actin and inhibits the polymerization at the barbed end, therefore contributes to the maintenance of the intracellular pool of polymerization competent ATP-G-actin. Cyclophosphamide (CP) is a cytostatic drug that can have potential side effects on muscle thin filaments at the level of actin in myofilaments. Here, we aimed at investigating the influence of CP on actin and its complexes with actin-binding proteins by using differential scanning calorimetry (DSC). We found that upon CP treatment, the denaturation of the Pro-G-actin and Lmod2-F-actin complexes was characterized by an increased enthalpy change. However, after the CP treatment, the melting temperature of F-actin was the same as in the presence of Lmod2, seems like Lmod2 does not have any effect on the structure of the CP alkylated F-actin. In case of Pro bound G-actin the melting temperature did not respond to the CP addition. The intracellular function of Lmod2 in muscle cells can be modified within CP drug treatment.

Keywords Actin · Profilin · Leiomodins2 · Cyclophosphamide · Differential scanning calorimetry

Introduction

The eukaryotic cytoskeleton is composed of different filament systems constructed by microtubules, intermediate filaments and actin-based microfilaments with their binding proteins. Actin plays an important role during muscle contraction as a dynamic component of the acto-myosin complex and in the motility, division, and transport processes of eukaryotic cells [1–7].

Cyclophosphamide (CP) is a chemotherapeutic drug with potential cytotoxic effects [8–13]. As it was previously shown with differential scanning calorimetry (DSC) scans, CP potentially affects the level of actin in muscle fibers [14–18]. Actin filaments can go through a cooperative and allosteric conformational change by ligand binding [19–23]. In the case of toxins it shows a concentration-dependent

effect [24, 25]. Previous studies have shown [15, 16, 26] that muscle thin filaments can be changed directly by the CP treatment [27]. Related to the expectations [13–17] a single dose of CP [28] already affects the structure of actin [29]. The actin monomer can bind adenosine nucleotide in a complex with divalent cations (Ca^{2+} or Mg^{2+}) in the cleft between the two main domains of the protein [30]. There is evolutionary importance of nucleotide-binding cleft of monomeric actin. It can advance a structural bridge between the two main domains if it links together the structural flexibility and the development of actin functions [31–35]. The interdomain linker plays a crucial role as an axis with the formation of two clefts between the domains and it can reduce the interdomain flexibility [36–41]. However, the upper cleft binds nucleotide and divalent cations. The transition of monomer to polymer form is based on a propeller-like rotation of domains with flattening of the subdomains in the monomer [40].

Members of the profilin family facilitate the nucleotide exchange on monomeric actin, inhibit the polymerization at the barbed end and contribute to the maintenance of the

✉ Dénes Lőrinczy
denes.lorinczy@aok.pte.hu

¹ Department of Biophysics, Medical School, University of Pécs, Szigeti str. 12, Pécs 7624, Hungary

polymerization competent intracellular ATP-G-actin pool [41–51]. Previous observations extend the functional variety of profilin as it can bind to lipids and to polyproline region [52, 53]. It has another important intracellular role in regulating the availability of free barbed ends and G-actin concentration via the regulation of actin polymerization rates [54, 55]. Altogether the interaction of profilin with ligands affects the F-actin scaffold formation and development thus the membrane structures (e.g., lamellipodia, filopodia or invadopodia) with influence on the cell motility [56]. Profilin overexpression in the case of malignant breast, hepatic and pancreatic cells reduces their motility. However, reduction in profilin level results in increased metastatic motility [57–60]. The role of profilin in cancer cells needs more investigation but the high expression of profilin in other types of cancers such as renal cell carcinoma [61] and gastric cancer [62] is correlated with the progression of the disease and poor patient outcomes [63].

Tropomodulin gene family members such as tropomodulin (Tmod) and leiomodulin (Lmod) play a role in the development of muscle sarcomeres [64]. Of interest, while Tmod1 localizes only to pointed ends toward the M-lines, Lmod2 shows diffuse distribution along the entire length of the thin filaments in rat cardio-myocytes [65, 66]. The expression of Lmod is increasing with myofibril maturation [67]. Deletion of striated muscle specific leiomodulin2 (Lmod2) caused dilated cardiomyopathy in juveniles [65, 68, 69] leading to unregulated sarcomeric actin dynamics and development. Surprisingly, in the case of cardiac cells originating from three-day old rats, leiomodulin can be found almost in the same amount as actin [67]. As it was previously shown Lmods bind directly to the sides of actin filaments and, besides the pointed end-binding related capping function, Lmod reduces the acto-myosin ATPase in vitro activity [70]. Both in vitro and in vivo results indicate that the function of Lmod is related to the regulation of the length of the thin filaments and the organization of sarcomere architecture [71–73].

As CP treatment has potential side effects on actin-based thin filaments in muscle, we hypothesized that these effects may be manifested through actin and/or actin-binding proteins. To test this possibility, in this work we aimed at investigating the effect of CP treatment on Pro or Lmod2 as abundant actin-binding proteins in muscle and their complexes with G- and F-actin, respectively.

Materials and methods

Profilin and leiomodulin2 expression and purification

The plasmid construction of His-tagged mouse profilin (Pro) (MW: 13.5 kDa) and *Rattus norvegicus* full-length cardiac

leiomodulin (Lmod2) (MW: 61.7 kDa) were expressed in *Escherichia coli* strains and purified as described previously [74, 70]. The concentration of Pro and Lmod2 was estimated at 280 nm with photometry (Jasco V-550 spectrophotometer) by using a calculated absorption coefficient of $\epsilon_{\text{Pro}} = 1.472 \text{ mL (mg cm)}^{-1}$ and $\epsilon_{\text{Lmod2}} = 0.388 \text{ mL (mg cm)}^{-1}$, respectively. Proteins were stored in MOPS-buffer (2 mM MOPS, 0.2 mM ATP, 0.1 mM CaCl_2 , 0.1 mM β -mercaptoethanol, pH 7.4) at -80°C and were used within 2 months.

Actin preparation from rabbit skeletal muscle

Ca^{2+} -G-actin was prepared from acetone powder of rabbit skeletal muscle as described earlier by Spudich and Watt [75] and stored in MOPS buffer. Actin concentration was determined from the absorption spectra (Jasco V-550 spectrophotometer) ($\epsilon_{\text{actin}} = 1.11 \text{ mL (mg cm)}^{-1}$ at 280 nm and $\epsilon_{\text{actin}} = 0.63 \text{ mL (mg cm)}^{-1}$ at 290 nm). We applied 2 mM EGTA and then 2 mM MgCl_2 treatment to exchange the bound calcium for magnesium on 2 mg/ml actin monomers. Actin polymerization was initiated by 100 mM KCl addition.

Cyclophosphamide treatment

For in vitro measurements applied dosage of cyclophosphamide (CP) was set to be comparable to the human dosage (150 mg kg^{-1} body mass) [9–12]. The average actin content of skeletal muscle is roughly 10% [75, 76] thus the average mass of Guinea pig gastrocnemius muscle (from our previous study [26]) is divided by 10 then by the mass of CP passed in the muscle ($150 \text{ mg kg}^{-1} \times \frac{\text{Mass of gastrocnemius}}{\text{Mass of the body}}$) resulted that the actin to CP ratio has to be $\frac{2000}{3}$ (it means 2 mg actin to 3 μg CP) as a single dose. However, as we used actin from rabbit skeletal muscle, we assume that the distribution of CP in rabbit skeletal muscle should be the same as in Guinea pig skeletal muscle. We carried out experiments—to achieve a more pronounced effect—with 5 times the dose of CP to treat actin followed by incubation at room temperature for 1 h.

DSC measurements

The measurements were started immediately after sample preparation. Data were collected by a SETARAM MicroDSCII calorimeter between 0 and 100°C with a heating rate of 0.3 K min^{-1} in conventional Hastelloy batch vessels ($V_{\text{max}} = 1 \text{ mL}$) to investigate denaturation with 950 μL sample volume (sample + buffer) in average. Sample and reference masses were identical with a precision of $\pm 0.1 \text{ mg}$, between 920 and 970 mg; this way the vessels' heat capacity was neglectable. MOPS buffer was used as a reference. With

the help of a two-point SETARAM peak integration setting, calorimetric enthalpy was calculated from the area under the heat absorption curve, and then, the results [denaturation or melting temperature (T_m) and calorimetric enthalpy data (ΔH_{cal})] (Table 1) were compared.

Results

The difference of nearly 1 °C in the melting temperature (T_m) can be considered significant in the case of thermal denaturation of biological samples; furthermore, it is generally accepted. Nevertheless, the T_m value of the process, one of the main characteristics of DSC curves, shows high accuracy and relatively low standard error.

All proteins were applied in a 2 mg mL⁻¹ concentration that corresponds to the ratio of 1:1.4 by 32.4 μM Lmod2 to 46 μM F-actin (~98% of Lmod2 was estimated in complex, $K_d = 230$ nM [77]) and 1:0.35 ratio by 133 μM Pro to 46 μM G-actin (~34% of Pro was in the complex, $K_d = 100$ nM [55]).

The Lmod2 as a mainly intrinsically disordered protein (IDP) [70] shows multiple transitions between 40 and 90 °C (Fig. 1A). The first point of the curve was shifted by -8 °C after the CP treatment, CP addition increased the height of the peaks between 4 and 55 °C, and decreased it in the range of 55–90 °C. The CP addition caused a 10% total enthalpy change (Table 1). The T_m of F-actin was increased by Lmod2 binding from 66 to 68.4 °C and the enthalpy was increased by 12% (Fig. 1B). However, the CP treatment increased the T_m of F-actin from 66 to 67.2 °C (Fig. 1C) and the enthalpy was increased by 16% (Table 1). For the comparison, the Lmod2 binding (Fig. 1D) also increased the T_m and the enthalpy (Table 1). DSC curves showed minor differences in T_m after the CP treatment; in case of Lmod2 bound F-actin it was decreased from 68.4 to 67.4 °C by 12% increase in

enthalpy (Fig. 1E) (Table 1). However, in the presence or absence of Lmod2 the T_m of CP treated F-actin was nearly identical ~67 °C but the enthalpy was increased by 11% in case of Lmod2 bound F-actin (Table 1) (Fig. 1F).

The T_m of Pro denaturation seems to be independent of CP treatment, it was around 53.7 °C only the enthalpy was increased by 14% upon the addition of chemotherapeutic drug (Table 1) (Fig. 2A). The T_m of G-actin was found to be 58.3 °C (Fig. 2C) but in the presence of Pro it was decreased to 49.9 °C, and the CP caused its negligible reduction to 49.4 °C while the enthalpy was increased by 20% (Table 1) (Fig. 2B). Upon CP treatment, the T_m of G-actin was 58.8 °C and 49.4 °C in the absence and presence of Pro, respectively, the enthalpy was increased by ~12% (Table 1) (Fig. 2D).

Discussion

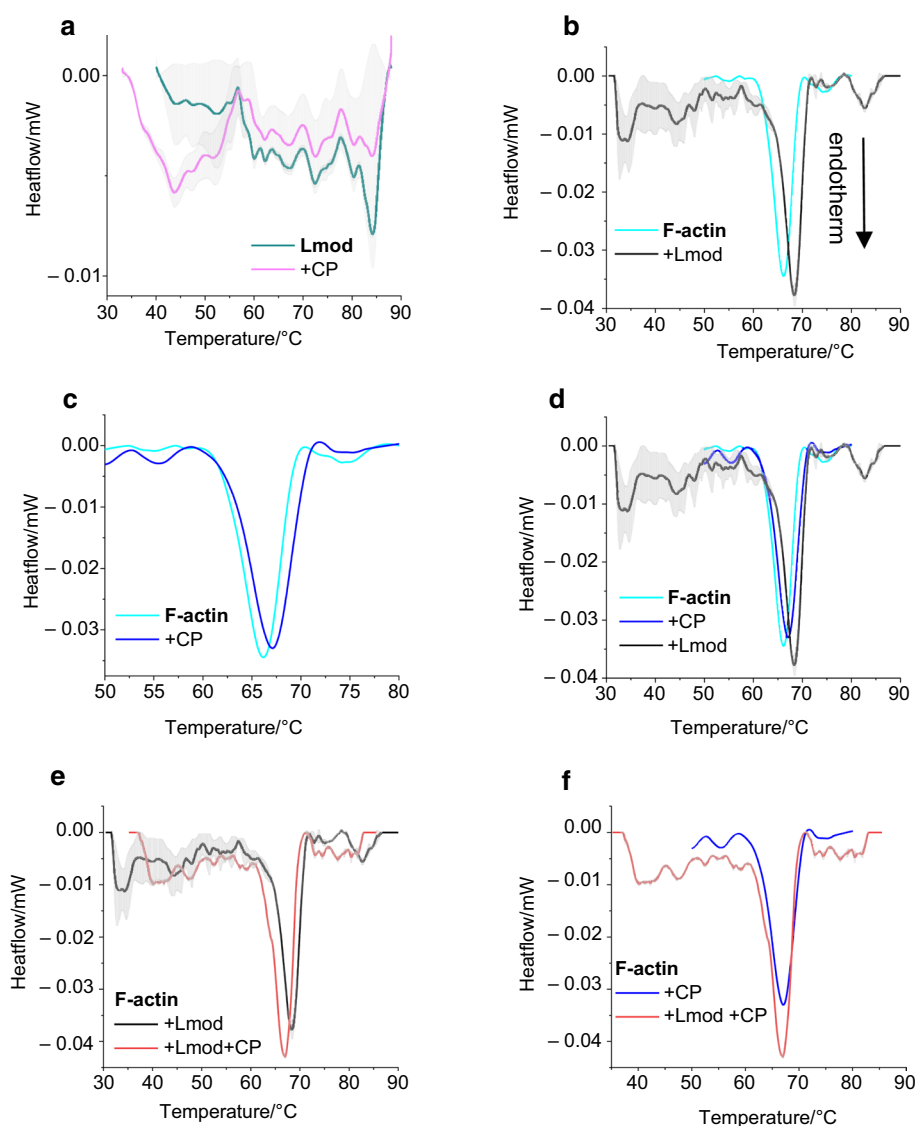
The shape of DSC graphs and the quantitative analysis; the denaturation temperatures with the calorimetric enthalpy clearly indicate the significance of the CP effect. In the case of F-actin it is manifested in a lower denaturing temperature and a higher enthalpy change in the presence of Lmod2. Although, in the absence of Lmod2 both parameters were increased upon CP treatment. Lmod2 binding can result in a structural alteration of the filaments as indicated by the increased denaturing temperature and enthalpy. In contrast with our previous data the relative FRET transfer efficiency in the case of double-labeled filaments was increased by Lmod2 binding [70]. The increased FRET transfer can be interpreted as Lmod2 bound filaments being more flexible but the increased denaturing temperature and enthalpy belong to a more compacted structure. We presume that the 'open gate' conformation model can describe the difference, as the donor fluorophores are turned to be more exposed by Lmod2 binding and their emission shows a steep reduction

Table 1 Thermal parameters of the denaturation of different native and CP treated G-, or F-actin and their complexes with actin-binding proteins as Lmod2 or Pro

Thermal parameters						
	T_m /°C	ΔH_{cal} /J/g		T_m /°C	ΔH_{cal} /J/g	
G-actin			F-actin			
Native	58.3 ± 0.028	0.041 ± 0.007	Native	66 ± 0.011	0.032 ± 0.009	
CP treated	58.8 ± 0.012	0.042 ± 0.005	CP treated	67.2 ± 0.037	0.037 ± 0.005	
With pro	49.9 ± 0.045	0.038 ± 0.009	With Lmod	68.4 ± 0.013	0.036 ± 0.006	
With pro, CP treated	49.4 ± 0.015	0.047 ± 0.012	With Lmod, CP treated	67.4 ± 0.01	0.041 ± 0.0102	
Pro			Lmod			
Native	53.8 ± 0.011	0.056 ± 0.007	Native (Multiple peaks)	40–55	55–90	0.33 ± 0.008
CP treated	53.6 ± 0.022	0.064 ± 0.005	CP treated (Multiple peaks)	32–55	55–90	0.033 ± 0.009

Data are presented as average ± standard deviation (SD) of three different measurements. The calorimetric enthalpy (ΔH_{cal}) refers to the whole denaturation range and is normalized by the sample mass. T_m melting temperature, ΔH_{cal} calorimetric enthalpy

Fig. 1 The effect of Lmod2 on the thermal denaturation of CP-modified F-actin. **A** The denaturation curves of 32.4 μM Lmod2 in the absence (green line) or in the presence of 15 $\mu\text{g mL}^{-1}$ CP (magenta line). **B** DSC scans of 46 μM F-actin in the absence (cyan line) or in the presence of 32.4 μM Lmod2 in 1:1.4 ratio (black line). **C** The denaturation of F-actin in the absence (cyan line) or in the presence of CP (blue line). **D** For the comparison, the denaturation of F-actin in the absence (cyan line), in the presence of Lmod2 (black line), or in the presence of CP (blue line). **E** DSC scan of Lmod2 decorated F-actin (black line) and of sample treated with CP (red line). **F** The thermal response of CP treated F-actin in the absence (blue line) or in the presence of Lmod2 (red line). The scans are average of three measurements with the gray fields indicated \pm standard deviation (SD) and the endotherm effect is deflected downward. (Color figure online)



by the temperature, and thus increasing the value of energy transfer efficiency [64]. According to our working model, Lmod2 decorated filaments (Fig. 3A) act like stiff rods with a couple of well exposed free sites on the side of filamentous actin (indicated by black arrows in Fig. 3A). Interestingly, the mainly intrinsically disordered chains of Lmod2 show some sensitivity to the CP treatment. Presumably, the CP can directly affect the structure of actin monomers and thus can result in similar thermal stability and somewhat higher enthalpy change than in the absence of Lmod2, the CP alkylated nucleotide-binding residues of monomers can result in the majority of structural changes in the filaments [27 – 29] and coupled with a minor enthalpy change by Lmod2 binding.

In the case of G-actin, the CP-modified thermodynamic stability can be linked to a higher denaturing temperature. However, subdomains of actin monomers can be arranged to

a less stable structure by Pro binding. Referring to the PDB ID: 2BTF structure [78], the Pro binds between the subdomain 1 and 3. Although we can expect that the Pro stabilizes the structure of the monomer thus leading to higher denaturing temperature, our data shows the opposite in good agreement with a previous study [51]. It was interpreted (Fig. 3B) as the cooperativity of the thermal unfolding within Pro binding was increased while the thermodynamic stability of the actin monomer was decreased (black arrows on Fig. 3B) [51]. We assume that the local dynamics of the subdomains is important for the binding of actin-binding proteins and do not directly affect the global thermodynamic stability of the actin monomer's structure. All these observations fit in the idea of Levitsky, as well as they were modeling the thermal stability of G-actin which was increased when the nucleotide-binding cleft is closed and decreased if it was open [79]. This seems like the thermodynamic stability of

Fig. 2 The effect of Pro on thermal denaturation of CP-modified G-actin. **A** The denaturation curves of 133 μM Pro in the absence (green line) or in the presence of 15 $\mu\text{g mL}^{-1}$ CP (magenta line). **B** DSC scans of 46 μM G-actin in the presence of 133 μM Pro in 0.35:1 ratio (black line) and of sample treated with 15 $\mu\text{g mL}^{-1}$ CP (red line). **C** Denaturation curve of G-actin (cyan line) in the absence and in the presence of Pro (black line). **D** The DSC curves of CP treated G-actin in the absence (blue line) and in the presence of Pro (red line). The scans are average of three measurements with the gray fields indicated \pm SD and endotherm effect is deflected downward. (Color figure online)

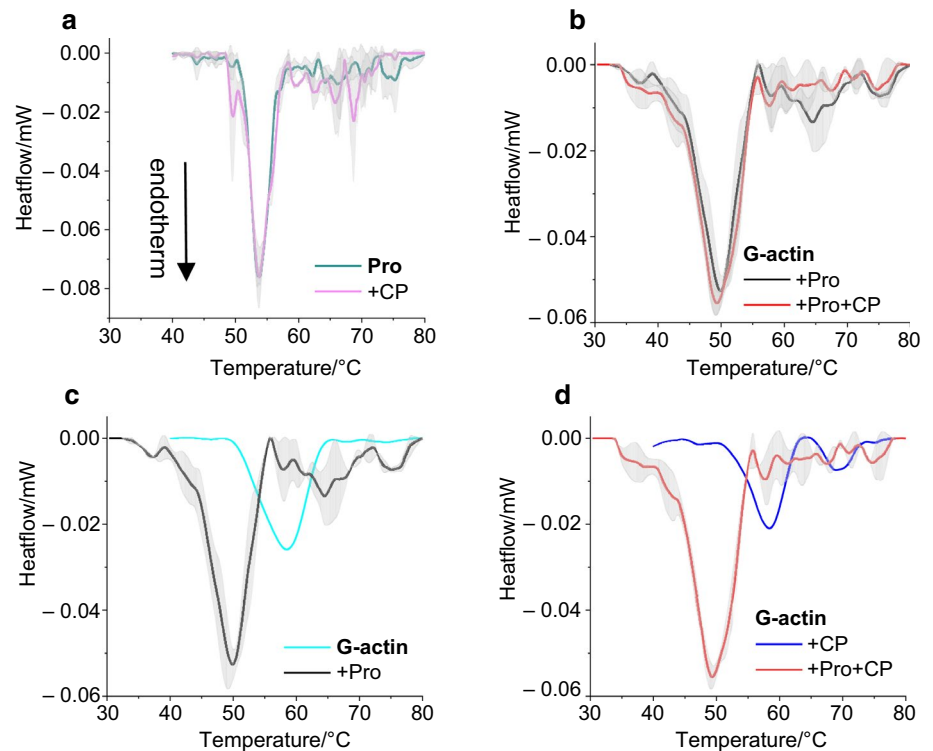
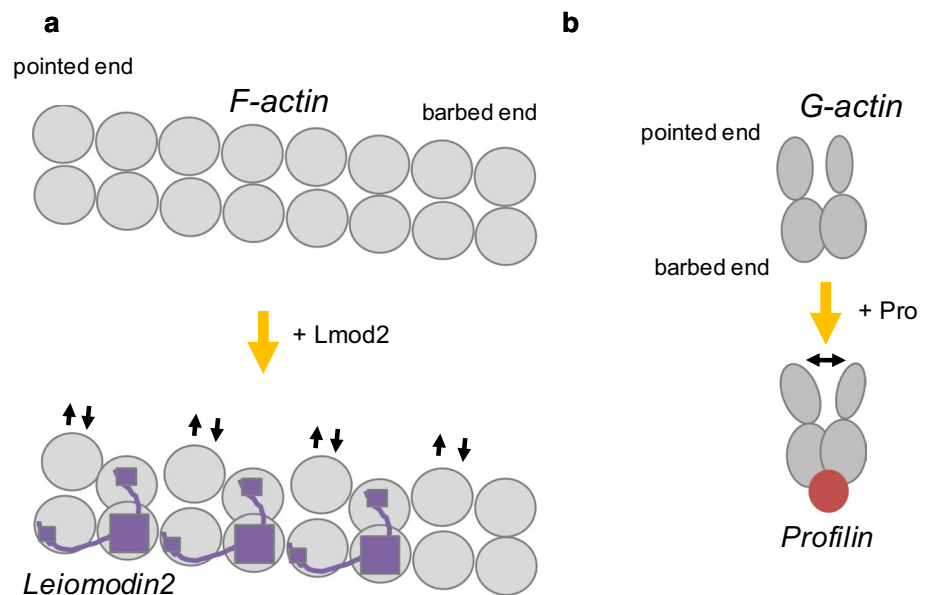


Fig. 3 Schematic model of the effect of Lmod2 on F-actin, and Pro on G-actin



monomeric actin can be affected by the conformation of the nucleotide-binding cleft and subdomains can be independent of the global thermodynamic stability of actin [28]. However, the only direct response of Pro to the CP treatment was the increased enthalpy change while the enthalpy of actin in the absence of Pro was increased as well. The Pro binding reduced stability of monomer structure looks insensitive to the CP treatment caused alkylation [27–29].

Conclusions

With the development of muscle tissues, the maturation of the filamentous actin system in sarcomeres requires the functional coordination of several different binding proteins. The drug treatment can modify the complex machinery of monomeric and filamentous actin rearrangement. Here, we have

shown that actin-binding proteins can modify the response of actin to the CP treatment. The Pro and Pro-G-actin complex reacted to the CP addition only by enthalpy change. This indicates that CP does not have any major effect on the structure and function of Pro and its complex with G-actin. Related to the increased thermal parameters of F-actin in the presence of CP, seems like the CP treatment advanced their stability. In the case of Lmod2 and Lmod2-decorated filamentous actin, the CP treatment influenced both parameters as reduced melting temperature and increased enthalpy change. These effects can be the result of structural modifications of Lmod2 leading to a weakened binding strength/functionality.

In summary, the Lmod2-related development of muscle cells can be modified by CP treatment. On the other hand, Pro seems to be insensitive to the CP treatment.

Acknowledgements This work was supported by CO-272 (OTKA) grant (DL) and supported by University of Pécs, Medical School, grant of Dr. Szolcsányi János Research Fund (ÁOK-KA) (DS).

Authors' contributions Dávid Szatmári was involved in rising the problem. Dávid Szatmári, Beáta Bugyi and Réka Pintér were involved in sample preparation and handling. Dávid Szatmári, Beáta Bugyi and Dénes Lőrinczy were involved in data analysis and manuscript writing. Dénes Lőrinczy was the corresponding author and also principal investigator and did DSC experiments.

Funding Open access funding provided by University of Pécs.

Availability of data and material There are no additional available data to upload.

Declarations

Conflicts of interests The authors declare that they have no known competing financial interests or personal relationships that could have appeared to influence the work reported in this paper.

Consent for publication Copyright form has been uploaded with the manuscript.

Open Access This article is licensed under a Creative Commons Attribution 4.0 International License, which permits use, sharing, adaptation, distribution and reproduction in any medium or format, as long as you give appropriate credit to the original author(s) and the source, provide a link to the Creative Commons licence, and indicate if changes were made. The images or other third party material in this article are included in the article's Creative Commons licence, unless indicated otherwise in a credit line to the material. If material is not included in the article's Creative Commons licence and your intended use is not permitted by statutory regulation or exceeds the permitted use, you will need to obtain permission directly from the copyright holder. To view a copy of this licence, visit <http://creativecommons.org/licenses/by/4.0/>.

References

- Cossart P. Actin-based bacterial motility. *Curr Opin Cell Biol.* 1996;7:94–101.
- Steinmetz MO, Stoffler D, Hoenger A, Bremer A, Aebi U. Actin: from cell biology to atomic detail. *J Struct Biol.* 1997;119:295–320.
- Pollard TD, Blanchoin L, Mullins RD. Molecular mechanisms controlling actin filament dynamics in nonmuscle cells. *Ann Rev Biophys Biomol Struct.* 2000;29:545–76.
- Pollard TD, Borisy GG. Cellular motility driven assembly and disassembly of actin filaments. *Cell.* 2003;112:453–65.
- Carlier M-F, Le Clainche C, Wiesner S, Pantolini D. Actin-based motility: from molecules to movement. *BioEssays.* 2003;25:336–45.
- Pantolini D, Le Clainche C, Carlier M-F. Mechanism of actin-based motility. *Science.* 2001;292:1502–6.
- Hehny H, Stammes M. Regulating cytoskeleton-based vesicle motility. *FEBS Lett.* 2007;581:2112–8.
- WHO Model List of Essential Medicines. 2015; http://www.who.int/selection_medicines/committees/expert/20/EML_2015_FINAL_amended_JUN2015.pdf?ua=1.
- Notermans NC, Lokhorst HM, Franssen H, Van der Graaf Y, Teunissen LL, Jennekens FG, Van den Berg LH, Wokke JH. Intermittent cyclophosphamide and prednisone treatment of polyneuropathy associated with monoclonal gammopathy of undetermined significance. *Neurology.* 1996;47(5):1227–33.
- Hamidou MA, Belizna C, Wiertelowsky S, Audrain M, Biron C, Grolleau JY, Mussini JM. Intravenous cyclophosphamide in refractory polyneuropathy associated with IgM monoclonal gammopathy: uncontrolled open trial. *Am J Med.* 2005;118(4):426–30.
- Kemp G, Rose P, Lurain J, Berman M, Manetta A, Roulet B, Homesley H, Belpomme D, Glick J. Amifostine pretreatment for protection against cyclophosphamide-induced and cisplatin-induced toxicities: results of a randomized control trial in patients with advanced ovarian cancer. *J Clin Oncol.* 1996;14:2101–12.
- Spitzer TR, Cirenza E, McAfee S, Foelber R, Zarzin J, Cahill R, Mazumder A. Phase I-II trial of high-dose cyclophosphamide, carboplatin and autologous bone marrow or peripheral blood stem cell rescue. *Bone Marrow Transpl.* 1995;15:537–42.
- Tschöp K, Rommel F, Schmidkonz P, Emmerich B, Schulze J. Neuropathy after cyclophosphamide high dose chemotherapy in a Morbus Werlhof patient. *Deutsche Med Wisch.* 2001;126(12):T17–20.
- Könczöl F, Wiegand N, Nót LG, Lőrinczy D. Examination of the cyclophosphamide-induced polyneuropathy on guinea pig sciatic nerve and gastrocnemius muscle with differential scanning calorimetry. *J Thermal Anal Calorim.* 2014;115:2239–43.
- Lőrinczy D. Investigation of side effects in polyneuropathy on skeletal muscle by DSC caused by cyclophosphamide treatment. *Eur Biophys J.* 2019;48(Suppl. 1):S238.
- Lőrinczy D. Cyclophosphamide treatment evoked side effects on skeletal muscle monitored by DSC. *J Thermal Anal Calorim.* 2020;142:1897–901.
- Dergez T, Könczöl F, Farkas N, Belagyi J, Lőrinczy D. DSC study of glycerol-extracted muscle fibers in intermediate states of ATP hydrolysis. *J Thermal Anal Calorim.* 2005;80:445–9.
- Dergez T, Lőrinczy D, Könczöl F, Farkas N, Belagyi J. Differential scanning calorimetry study of glycerinated rabbit psoas muscle fibres in intermediate state of ATP hydrolysis. *BMC Struct Biol.* 2007;7:41–50.
- Drewes G, Faulstich H. Cooperative effects on filament stability in actin modified at the C-terminus by substitution or truncation. *Eur J Biochem.* 1993;212:247–53.
- Orlova A, Prochniewicz E, Egelman EH. Structural dynamics of F-actin: II. Cooperativity in structural transitions. *J Mol Biol.* 1995;245:598–607.

21. Orlova A, Egelman EH. Cooperative rigor binding of myosin to actin is a function of F-actin structure. *J Mol Biol.* 1997;265:469–74.
22. Moracewska J. Structural determinants of cooperativity in actomyosin interactions. *Acta Biochim Pol.* 2002;49:805–12.
23. Egelman EH. A tale of two polymers: new insights into helical filaments. *Nat Rev Mol Cell Biol.* 2003;4:621–30.
24. Visegrády B, Lőrinczy D, Hild G, Somogyi B, Nyitrai M. The effect of phalloidin and jaspaklinolide on the flexibility and thermal stability of actin filaments. *FEBS Lett.* 2004;565:163–6.
25. Visegrády B, Lőrinczy D, Hild G, Somogyi B, Nyitrai M. A simple model for the cooperative stabilisation of actin filaments by phalloidin and jaspaklinolide. *FEBS Lett.* 2005;579:6–10.
26. Farkas P, Könczöl F, Lőrinczy D. Examination of the peripheral nerve and muscle damage in cyclophosphamide monotherapy with DSC in animal models. *J Thermal Anal Calorim.* 2016;126:47–53.
27. Farkas P, Szatmári D, Könczöl F, Lőrinczy D. Cyclophosphamide treatment evoked side effect on skeletal muscle actin, monitored by DSC. *J Thermal Anal Calorim.* 2021. <https://doi.org/10.1007/s10973-021-10774-7>.
28. Szatmári D, Lőrinczy D. Alterations of inter domain flexibility in actin monomers reduced by cyclophosphamide treatment. *J Thermal Anal Calorim.* 2021. <https://doi.org/10.1007/s10973-021-11096-4>.
29. Lőrinczy D, Szatmári D. Dose-dependent effect of cyclophosphamide treatment on actin. *J Thermal Anal Calorim.* 2022. <https://doi.org/10.1007/s10973-022-11253-3>.
30. Sheterline P, Clayton J, Sparrow J. Actin Protein profile. 1995;2:1–103.
31. Muzzopappa F, Wilson A, Kirilovsky D. Interdomain interactions reveal the molecular evolution of the orange carotenoid protein. *Nat Plants.* 2019;5:1076–86.
32. Smock RG, Rivoire O, Russ WP, Swain JF, Leibler S, Ranganathan R, Gierasch LM. An interdomain sector mediating allostery in Hsp70 molecular chaperones. *Mol Syst Biol.* 2010;6:414.
33. Huang S, Cao J, Jiang M, Labesse G, Liu J, Pin JP, Rondard P. Interdomain movements in metabotropic glutamate receptor activation. *Proc Natl Acad Sci USA.* 2011;108:15480–5.
34. Vogel M, Mayer MP, Bukau B. Allosteric regulation of Hsp70 chaperones involves a conserved interdomain linker. *J Biol Chem.* 2006;281(50):38705–11.
35. Guaitoli G, Raimondi F, Gilsbach BK, Gómez-Llrente Y, Deyaert E, Renzi F, Li X, Schaffner A, Jagtap PK, Boldt K, von Zweyendorf F, Gotthardt K, Rimer DD, Yue Z, Burgin A, Janjic N, Sattler M, Versées W, Ueffing M, Ubarretxena-Belandia I, Kortholt A, Gloeckner CJ. Structural model of the dimeric Parkinson's protein LRRK2 reveals a compact architecture involving distant interdomain contacts. *Proc Natl Acad Sci USA.* 2016;113(30):4357–66.
36. Merino F, Pospich S, Funk J, Wagner T, Küllmer F, Hans-Dieter A, Bieling P, Raunser S. Structural transitions of F-actin upon ATP hydrolysis at near-atomic resolution revealed by cryo-EM. *Nat Struct Mol Biol.* 2018;25:528–37.
37. Wriggers W, Schulten K. Stability and dynamics of G-actin: backdoor water diffusion and behavior of a subdomain 3/4 loop. *Biophys J.* 1997;73:624–39.
38. Scipion CPM, Ghoshdastider U, Ferrer FJ, Yuen TY, Wongsantichon J, Robinson RC. Structural evidence for the roles of divalent cations in actin polymerization and activation of ATP hydrolysis. *Proc Natl Acad Sci USA.* 2018;115(41):10345–50.
39. Dominguez R, Holmes KC. Actin structure and function. *Ann Rev Biophys.* 2011;40:169–86. <https://doi.org/10.1146/annurev-biophys-042910-155359>. PMID:21314430;PMCID:PMC3130349.
40. Kang H, Bradley MJ, McCullough BR, Pierre A, Grintsevich EE, Reisler E, De La Cruz EM. Identification of cation-binding sites on actin that drive polymerization and modulate bending stiffness. *Proc Natl Acad Sci USA.* 2012;109(42):16923–7.
41. Mockrin SC, Korn ED. Acanthamoeba profilin interacts with G-actin to increase the rate of exchange of actin-bound adenosine 5'-triphosphate. *Biochem.* 1980;19:5359–62.
42. Pollard TD, Cooper JA. Quantitative analysis of the effect of Acanthamoeba profilin on actin filament nucleation and elongation. *Biochem.* 1984;23:6631–41.
43. Korenbaum E, Nordberg P, Bjorkegren Sjogren C, Schutt CE, Lindberg U, Karlsson R. The role of profilin in actin polymerization and nucleotide exchange. *Biochem.* 1998;37:9274–83.
44. Kovar DR, Kuhn JR, Tichy AL, Pollard TD. The fission yeast cytokinesis formin Cdc12p is a barbed end actin filament capping protein gated by profilin. *J Cell Biol.* 2003;161:875–87.
45. Kovar DR, Pollard TD. Progressing actin: formin as a processive elongation machine. *Nat Cell Biol.* 2004;6:1158–9.
46. Witke W. The role of profilin complexes in cell motility and other cellular processes. *Trends Cell Biol.* 2004;14(8):461–9.
47. Ding Z, Bae YH, Roy P. Molecular insights on context-specific role of profilin-1 in cell migration. *Cell Adhes Migr.* 2012;6(5):442–9.
48. Goldschmidt-Clermont PJ, Furman MI, Wachsstock D, Safer D, Nachmias VT, Pollard TD. The control of actin nucleotide exchange by thymosin beta 4 and profilin. A potential regulatory mechanism for actin polymerization in cells. *Mol Biol Cell.* 1992;3(9):1015–24.
49. Pollard TD, Borisov GG. Cellular motility driven by assembly and disassembly of actin filaments. *Cell.* 2003;112(4):453–65.
50. Paavilainen VO, Bertling E, Falck S, Lappalainen P. Regulation of cytoskeletal dynamics by actin-monomer-binding proteins. *Trends Cell Biol.* 2004;14(7):386–94.
51. Kardos R, Nevalainen E, Nyitrai M, Hild G. The effect of ADF/cofilin and profilin on the dynamics of monomeric actin. *Biochim et Biophys Act Prot Proteo.* 2013;1834(10):2010–9.
52. Bae YH, Ding Z, Das T, Wells A, Gertler F, Roy P. Profilin1 regulates PI(3,4)P2 and lamellipodin accumulation at the leading edge thus influencing motility of MDA-MB-231 cells. *Proc Natl Acad Sci USA.* 2010;107(50):21547–52.
53. Ding Z, Gau D, Deasy B, Wells A, Roy P. Both actin and polyproline interactions of profilin-1 are required for migration, invasion and capillary morphogenesis of vascular endothelial cells. *Exp Cell Res.* 2009;315(17):2963–73.
54. Rotty JD, Wu C, Haynes EM, Suarez C, Winkelman JD, Johnson HE, Haugh JM, Kovar DR, Bear JE. Profilin-1 serves as a gatekeeper for actin assembly by Arp2/3-dependent and -independent pathways. *Dev Cell.* 2015;32(1):54–67.
55. Pernier J, Shekhar S, Jegou A, Guichard B, Carlier MF. Profilin interaction with actin filament barbed end controls dynamic instability, capping, branching, and motility. *Dev Cell.* 2016;36(2):201–14.
56. Lorent G, Syriani E, Morales M. Actin filaments at the leading edge of cancer cells are characterized by a high mobile fraction and turnover regulation by profilin I. *PLoS One.* 2014;9(1):85817.
57. Janke J, Schluter K, Jandrig B, Theile M, Kolble K, Arnold W, Grinstein E, Schwartz A, Estevez-Schwarz L, Schlag PM, Jockusch BM, Scherneck S. Suppression of tumorigenicity in breast cancer cells by the microfilament protein profilin I. *J Exp Med.* 2000;191(10):1675–86.
58. Roy P, Jacobson K. Overexpression of profilin reduces the migration of invasive breast cancer cells. *Cell Motil Cytoskeleton.* 2004;57(2):84–95.
59. Wang W, Goswami S, Lapidus K, Wells AL, Wyckoff JB, Sahai E, Singer RH, Segall JE, Condeelis JS. Identification and testing of a gene expression signature of invasive carcinoma cells within primary mammary tumors. *Cancer Res.* 2004;64(23):8585–94.
60. Schoppmeyer R, Zhao R, Cheng H, Hamed M, Liu C, Zhou X, Schwarz EC, Zhou Y, Knorck A, Schwarz G, Ji S, Liu L, Long J, Helms V, Hoth M, Yu X, Qu B. Human profilin 1 is a negative

- regulator of CTL mediated cell-killing and migration. *Eur J Immunol.* 2017;47(9):1562–72.
61. Karamchandani JR, Gabril MY, Ibrahim R, Scorilas A, Filter E, Finelli A, Lee JY, Ordon M, Pasic M, Romaschin AD, Yousef GM. Profilin-1 expression is associated with high grade and stage and decreased disease-free survival in renal cell carcinoma. *Hum Pathol.* 2015;46(5):673–80.
 62. Cheng YJ, Zhu ZX, Zhou JS, Hu ZQ, Zhang JP, Cai QP, Wang LH. Silencing profilin-1 inhibits gastric cancer progression via integrin beta1/focal adhesion kinase pathway modulation. *World J Gastroenterol.* 2015;21(8):2323–35.
 63. Coumans JVF, Davey RJ, Moens PDJ. Cofilin and profilin: partners in cancer aggressiveness. *Biophys Rev.* 2018;10(5):1323–35. <https://doi.org/10.1007/s12551-018-0445-0>.
 64. Tolkathev D, Gregorio CC, Kostyukova AS. The role of leiomodin in actin dynamics: a new road or a secret gate. *FEBS J.* 2022. <https://doi.org/10.1111/febs.16128>.
 65. Tsukada T, Pappas CT, Moroz N, Antin PB, Kostyukova AS, Gregorio CC. Leiomodin-2 is an antagonist of tropomodulin-1 at the pointed end of the thin filaments in cardiac muscle. *J Cell Sci.* 2010;123(18): 3136–45. Epub 2010/08/26. pmid:20736303.
 66. Boczkowska M, Rebowski G, Kremneva E, Lappalainen P, Dominguez R. How Leiomodin and Tropomodulin use a common fold for different actin assembly functions. *Nat Commun.* 2015;6:8314. pmid:26370058.
 67. Skwarek-Maruszewska A, Boczkowska M, Zajac AL, Kremneva E, Svitkina T, Dominguez R, Lappalainen P. Different localizations and cellular behaviors of leiomodin and tropomodulin in mature cardiomyocyte sarcomeres. *Mol Biol Cell.* 2010;21(19):3352–61.
 68. Pappas CT, Mayfield RM, Henderson C, JAMILPOUR N, Cover C, Hernandez Z, et al. Knockout of Lmod2 results in shorter thin filaments followed by dilated cardiomyopathy and juvenile lethality. *Proc Natl Acad Sci USA.* (2015);112(44):13573–8. pmid:26487682.
 69. Li S, Mo K, Tian H, Chu C, Sun S, Tian L, et al. Lmod2 piggyBac mutant mice exhibit dilated cardiomyopathy. *Cell Biosci.* 2016;6:38. Epub 2016/06/09. pmid:27274810.
 70. Szatmári D, Bugyi B, Ujfalusi Z, Grama L, Dudás R, Nyitrai M (2017) Cardiac leiomodin2 binds to the sides of actin filaments and regulates the ATPase activity of myosin. *PLoS ONE.* 2017;12(10):e0186288. <https://doi.org/10.1371/journal.pone.0186288>.
 71. Kiss B, Gohlke J, Tonino P, Hourani Z, Kolb J, Strom J, Alekhina O, Smith JE, Ottenheijm C, Gregorio C, Granzier H. Nebulin and Lmod2 are critical for specifying thin-filament length in skeletal muscle. *Sci Adv.* 2020;6:1992.
 72. Wang Z, Grange M, Pospich S, Wagner T, Kho AL, Gautel M, Raunser S. Structures from intact myofibrils reveal mechanism of thin filament regulation through nebulin. *Sci.* 2022;18(375):6582. <https://doi.org/10.1126/science.abn1934>.
 73. Szikora S, Görög P, Mihály J. The mechanisms of thin filament assembly and length regulation in muscles. *Int J Mol Sci.* 2022;23:5306.
 74. Kardos R, Pozsonyi K, Nevalainen E, Lappalainen P, Nyitrai M, Hild G. The effects of ADF/cofilin and profilin on the conformation of the ATP-binding cleft of monomeric actin. *Biophys J.* 2009;96:2335–43.
 75. Spudich JA, Watt S. The regulation of rabbit skeletal muscle contraction I Biochemical studies of the interaction of the tropomyosin-troponin complex with actin and the proteolytic fragments of myosin. *J Biol Chem.* 1971;246(15):4866–71.
 76. Szikora S, Gajdos T, Novák T, Farkas D, Földi I, Lenart P, Erdélyi M, Mihály J. Nanoscopy reveals the layered organization of the sarcomeric H-zone and I-band complexes. *J Cell Biol.* 2020. <https://doi.org/10.1083/jcb.201907026>.
 77. Chen X, Ni F, Kondrashkina E, Ma J, Wang Q. Mechanisms of leiomodin 2-mediated regulation of actin filament in muscle cells. *Proc Natl Acad Sci USA.* 2015;112(41):12687–92.
 78. Schutt CE, Myslik JC, Rozycki MD, Goonesekere NC, Lindberg U. The structure of crystalline profilin-beta-actin. *Nature.* 1993;365(6449):810–6.
 79. Levitsky DI, Pivovarova AV, Mikhailova VV, Nikolaeva OP. Thermal unfolding and aggregation of actin. *FEBS J.* 2008;275:4280–95.

Publisher's Note Springer Nature remains neutral with regard to jurisdictional claims in published maps and institutional affiliations.